Identification of Active Edge Sites for Electrochemical H₂ Evolution from MoS₂ Nanocatalysts

Thomas F. Jaramillo, Kristina P. Jørgensen, Jacob Bonde, Jane H. Nielsen, Sebastian Horch, Ib Chorkendorff k

The identification of the active sites in heterogeneous catalysis requires a combination of surface sensitive methods and reactivity studies. We determined the active site for hydrogen evolution, a reaction catalyzed by precious metals, on nanoparticulate molybdenum disulfide (MoS₂) by atomically resolving the surface of this catalyst before measuring electrochemical activity in solution. By preparing MoS₂ nanoparticles of different sizes, we systematically varied the distribution of surface sites on MoS₂ nanoparticles on Au(111), which we quantified with scanning tunneling microscopy. Electrocatalytic activity measurements for hydrogen evolution correlate linearly with the number of edge sites on the MoS₂ catalyst.

rogress in the field of heterogeneous catalysis is often hampered by the difficulty of identifying the active site on a catalyst surface (1, 2). In homogeneous catalysis, the active center is generally more clearly defined and quantified, with spectroscopic and mechanistic studies providing direct insight into reactive intermediates. Solid-state catalysts, however, commonly exhibit a variety of different surface sites that are difficult to identify and quantify; the scenario is further complicated when multiple sites work together in turning over a reaction. Identifying the most active site(s) is critical to designing and developing improved catalytic materials. Many useful in situ and ex situ experimental techniques, as well as computational methods, have been developed (3-5) to address this problem, but identifying the active site remains a challenging task.

In this study we used such methods to determine the active site of nanoparticulate MoS_2 for the hydrogen evolution reaction (HER), $2H^+ + 2e^- \rightarrow H_2$ (6, 7), which is fundamentally important for a variety of electrochemical processes, fuel cells (as the reverse reaction), and solar H_2 production (water splitting), particularly where there is a need to replace precious metal catalysts such as Pt (7, 8). In its bulk form, MoS_2 is a poor HER catalyst (9). Nanoparticulate MoS_2 , however, is a more promising system; density functional theory (DFT) calculations indicate that the edges of MoS_2 nanoparticles are active for hydrogen evolution (8), but no previous experiments have shown this conclusively.

Nanoparticulate MoS₂ has been studied previously in an attempt to link activity to specific

surface sites, in that MoS2 is used industrially as a hydrodesulfurization (HDS) catalyst (10, 11). Detailed insight has been gained from studies on simplified model systems in ultra-high vacuum (UHV) and by using computational methods (12-15), as well as from combining reactivity measurements and ex situ characterization of industrial catalyst samples (10, 11, 16). Structural studies on the MoS₂ catalyst have shown that it is composed almost entirely of flat polygons of S-Mo-S trilayers (10); depending on the synthesis conditions, these trilayers may stack in a graphite-like manner or remain as single trilayers. For single trilayers, two general kinds of surface sites exist-terrace sites, which are those on the basal plane, and edge sites, which lie at the edge of the nanoparticles. DFT studies suggest that the active site for HDS is on the edge of the MoS₂ nanoparticles. This result is supported by adsorption studies of thiophene using scanning tunneling microscopy (STM) (17). Despite numerous studies on this material, there is a call for studies that uniquely link the well-defined structures of the model system to catalytic activity under standard reaction conditions (18).

To provide an experimental elucidation of the active site for the HER, we prepared MoS₂ samples in UHV of deliberately chosen nanoparticulate morphologies such that the fractions of the terrace and edge sites were systematically varied, then characterized by STM. All of the MoS₂ samples in this study were synthesized on a clean Au(111) substrate by physical vapor deposition of Mo in a background of H₂S (19), followed by annealing, according to the approach in (13). Three samples were annealed at 400°C, two were annealed at 550°C, and a "blank" sample was synthesized without the deposition of Mo and annealed to 400°C. The Au(111) substrate serves to disperse the MoS₂ nanoparticles by its herringbone reconstruction and is not particularly active for the HER (20). To maintain discretely separated single trilayer particles, we purposely synthesized the samples with low area coverages of MoS2, less than onefourth ML (i.e., 0.25 nm²_{MoS2}/nm²_{geometric}).

Immediately after deposition, each sample was vacuum transferred to a second UHV chamber for STM imaging (Fig. 1). The crystallized, single-layered MoS₂ nanoparticles can be described as flat polygons with a conducting edge state, seen as bright lines along the particle perimeter. Comparison of representative images of samples annealed at 400°C (Fig. 1A) and 550°C (Fig. 1B) shows how particle size increased after sintering at the higher temperature. The particles annealed to 400°C are consistent with similarly prepared MoS2 nanoparticles on Au(111) (13). Besenbacher et al. have shown that the dominant edge structure of MoS₂ nanoparticles is that of a sulfided Mo edge and that this edge is particularly favored by larger-sized particles (12, 18). We also observe the predominance of the sulfided Mo-edge in our samples, regardless of annealing temperature. Thus, controlled sintering allows us to change the ratio of basal plane sites to edge sites without changing the nature of the edge. This sulfided $(1 \ 0 \ -1 \ 0)$

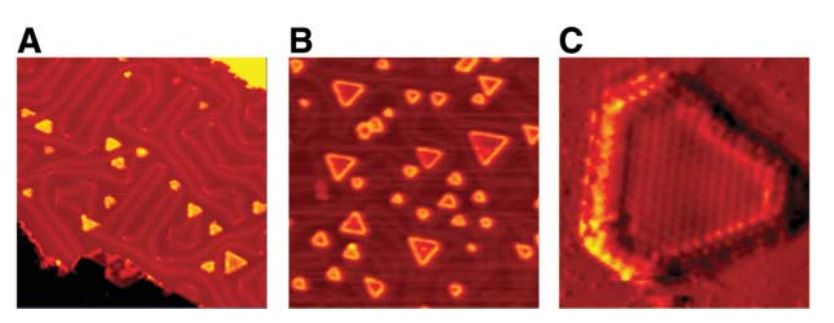


Fig. 1. A series of STM images of MoS₂ nanoparticles on Au(111). The particles exhibit the typical polygon morphology with conducting edge states and are dispersed on the Au surface irrespective of coverage and annealing temperature (400°C or 550°C). (**A**) Low coverage (0.06 nm²_{MoS2}/nm²_{geom.}), annealed to 400°C (470 Å by 470 Å, 1.2 nA, 4 mV). (**B**) High coverage (0.23 nm²_{MoS2}/nm²_{geom.}), annealed to 550°C (470 Å by 470 Å, 1.2 nA, 1.9 V). (**C**) Atomically resolved MoS₂ particle, from a sample annealed to 550°C, showing the predominance of the sulfided Mo-edge (19, 20) (60 Å by 60 Å, 1.0 nA, 300 mV).

¹Center for Individual Nanoparticle Functionality, Department of Physics, Nano-DTU, Technical University of Denmark, DK-2800 Lyngby, Denmark. ²Center for Atomic-scale Materials Design, Department of Physics, Nano-DTU, Technical University of Denmark, DK-2800 Lyngby, Denmark.

^{*}To whom correspondence should be addressed. E-mail: ibchork@fysik.dtu.dk

Mo-edge is the same structure predicted by DFT calculations to be the active site for H_2 evolution (8).

After imaging, we transfer the samples from UHV into an electrochemical cell to measure HER activity (21). Polarization curves (i - E) within a cathodic potential window, and corresponding Tafel plots (log i - E), are shown in

Fig. 2. Current densities are normalized to the geometric area of the exposed face of all samples.

The most inherent measure of activity for the HER is the exchange current density, i_0 (6, 7, 22, 23), which is determined by fitting i - E data to the Tafel equation (6), yielding Tafel slopes of 55 to 60 mV/decade and exchange current densities in the range of 1.3 ×

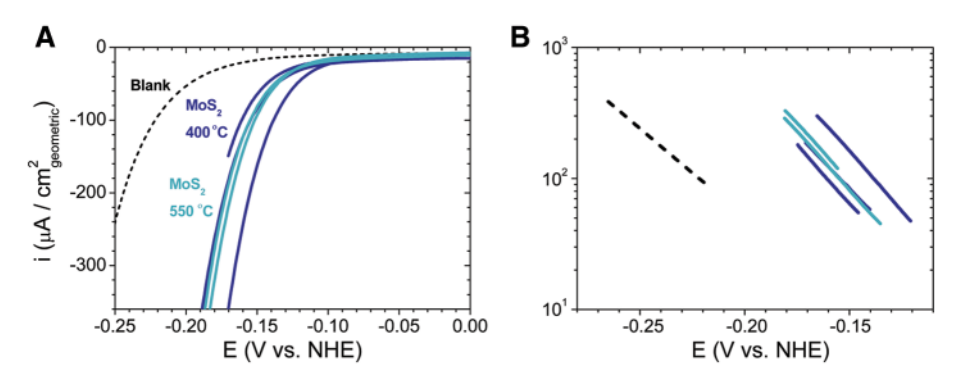


Fig. 2. Polarization curves and Tafel plots in a cathodic potential window for the five different MoS₂ samples as well as a blank sample. Samples annealed to 400°C are dark blue, samples annealed to 550°C light blue. (**A**) Polarization curve showing H₂ evolution on all samples. (**B**) Tafel plot (log current versus potential). All of the MoS₂ samples have Tafel slopes of 55 to 60 mV per decade irrespective of annealing temperature and coverage. Sweep rate: 5 mV/s.

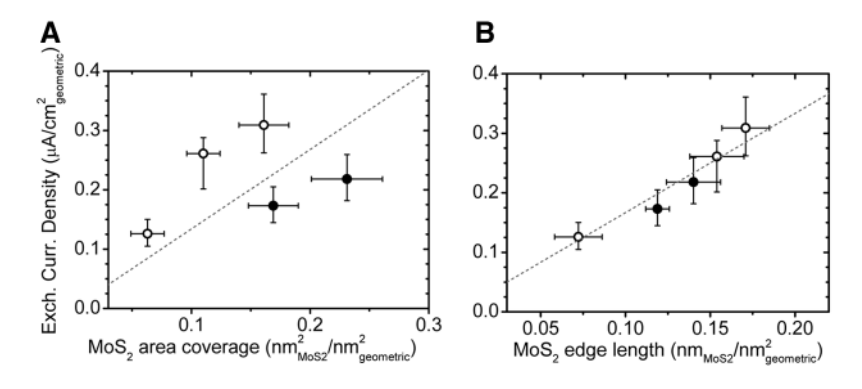
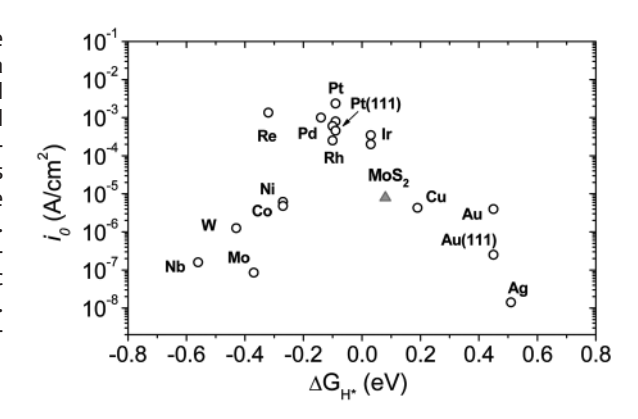


Fig. 3. Exchange current density versus (**A**) MoS₂ area coverage and (**B**) MoS₂ edge length. In both figures, open circles are samples annealed to 400°C, filled circles are samples annealed to 550°C. The exchange current density does not correlate with the area coverage of MoS₂, whereas it shows a linear dependence on the MoS₂ edge length. Exchange current densities are extracted from the Tafel plot in Fig. 2. The edge length was measured on all imaged particles and normalized by the imaged area.

Fig. 4. Volcano plot of the exchange current density as a function of the DFT-calculated Gibbs free energy of adsorbed atomic hydrogen for nanoparticulate MoS₂ and the pure metals (23). As seen, MoS₂ follows the same trend as the pure metals. The MoS₂ exchange current density is normalized to the atomic site density of Pt for comparison. Samples are polycrystalline unless otherwise noted.



 10^{-7} to 3.1×10^{-7} A/cm²_{geometric} for all MoS₂ samples (table S1). In Fig. 3, we plot the exchange current density for each sample versus two sample parameters, the MoS₂ area coverage (Fig. 3A), and the MoS₂ edge state length (Fig. 3B). The data points fall on a straight line only when plotted versus edge length. Although the points show some scatter around this trend, they are described by a best-fit linear relation with a slope of 1.67×10^{-20} A/nm_{MoS2-edge}.

Because the rate of reaction is directly proportional to the number of edge sites for all samples, regardless of particle size, we conclude that the edge site is indeed the active site (24). Bearing this in mind, we note in Fig. 3A that the exchange current densities of the samples sintered at 550°C are significantly lower than those prepared at 400°C, per MoS₂ coverage, exactly as one would expect considering that the sintered samples have less edge length per area of MoS₂.

We also compared nanoscale MoS_2 to other materials that catalyze the HER on a per active site basis (1). For this direct site-to-site comparison, we used the 1.5×10^{15} sites/cm² for the Pt(111) face as the basis for comparison as Pt is the archetypical HER catalyst (25). An exchange current density of 4.5×10^{-4} A/cm² for this face (26) yields a turnover frequency (TOF) of 0.9 s^{-1} (table S2). In general, TOFs of transition metals range over 10 orders of magnitude (Hg, for instance, has a TOF as low as $\sim 10^{-9} \text{ s}^{-1}$) (22). Given the slope in Fig. 3B, we have calculated the TOF of the MoS_2 edge to be 0.02 s^{-1} , indeed in the high range of TOFs for metals.

For further insight into the catalytic nature of the MoS₂ edge, we have added our data for nanoparticulate MoS₂ to a recent version of the volcano-type relations observed for HER catalysts (Fig. 4), in this case for the Gibbs free energy for atomic hydrogen adsorption (ΔG_H) (22, 23). These volcano relations ultimately reflect the Sabatier principle, which accounts for optimal surfaces as ones that exhibit moderate binding energies of reaction intermediates, hydrogen adsorption in the case of the HER. In Fig. 4, the exchange current density is shown as a function of the DFT-calculated free energy of adsorption of hydrogen, which was recently determined to be +0.08 eV for the MoS₂ edge (8). To add MoS₂ to this figure, we converted the TOF of nanoparticulate MoS2 to its exchange current density per 1.5 × 10¹⁵ sites/cm², which yields 7.9×10^{-6} A/cm² (table S2). This value surpasses those of the common metals and lies just below those of the precious Pt-group metals. When plotting this experimentally determined activity of the edge site versus its DFT-calculated $\Delta G_{\rm H}$ (8), we see that it follows the volcano trend (23). This agreement validates the predictive capability of this DFT model as well as its applicability beyond metal catalysts.

After identifying the active site and comparing it with typical metal catalysts, we may

consider how to improve its activity. The DFTcalculated ΔG_H of the MoS₂ edge site is slightly positive at +0.08 eV, with calculations suggesting an H coverage of only one-quarter on the edge under operating conditions (8). Thus, only 1 in 4 edge atoms evolves molecular H₂ at a given time, unlike Pt(111) which operates at a H-coverage of \sim 1 ML (7, 26, 27). If all MoS₂ edge sites could be made to adsorb H, activity could be increased by a factor of 4. This might be accomplished by appropriately tuning the electronic structure of the edge to increase the bond strength of the adsorbed H (23). Such a modification could simultaneously improve the inherent turnover of each edge site, further improving the overall activity of the material toward that of Pt-group metals.

References and Notes

- 1. G. A. Somorjai, Introduction to Surface Chemistry and Catalysis (Wiley, New York, 1994).
- 2. T. Zambelli, J. Wintterlin, J. Trost, G. Ertl, Science 273, 1688 (1996).
- 3. C. T. Campbell, Science 294, 1471 (2001).
- 4. N. I. Jaeger, Science 293, 1601 (2001).
- 5. S. Dahl et al., Phys. Rev. Lett. 83, 1814 (1999).
- 6. 1. O. M. Bockris, S. U. M. Khan, Surface Electrochemistry: A Molecular Level Approach. (Plenum, New York, 1993).
- 7. B. E. Conway, B. V. Tilak, Electrochim. Acta 47, 3571 (2002).

- 8. B. Hinnemann et al., J. Am. Chem. Soc. 127, 5308 (2005).
- 9. W. Jaegermann, H. Tributsch, Prog. Surf. Sci. 29, 1 (1988).
- 10. H. Topsøe, B. S. Clausen, F. E. Massoth, in Catalysis Science and Technology, J. R. Anderson, M. Boudart, Eds. (Springer-Verlag, New York, 1996), vol. 11.
- 11. R. R. Chianelli et al., Catal. Rev. 48, 1 (2006).
- 12. M. V. Bollinger et al., Phys. Rev. Lett. 87, 19 (2001).
- 13. S. Helveg et al., Phys. Rev. Lett. 84, 951 (2000).
- 14. J. Kibsgaard et al., J. Am. Chem. Soc. 128, 13950 (2006). 15. M. V. Bollinger, K. W. Jacobsen, J. K. Nørskov, Phys. Rev.
- B 67, 085410 (2003).
- 16. R. Prins, V. H. J. de Beer, G. A. Somorjai, Catal. Rev. Sci. Eng 31, 1 (1989).
- 17. J. V. Lauritsen et al., J. Catal. 224, 94 (2004).
- 18. J. V. Lauritsen et al., Nat. Nanotech. 2, 53 (2007).
- 19. Materials and methods are available as supporting material on Science Online.
- 20. J. Perez, E. R. Gonzalez, H. M. Villullas, J. Phys. Chem. B 102, 10931 (1998).
- 21. The cell, specifically designed for studies on UHVtransferred samples, is sealed upon the imaged (111) face of the sample with a viton o-ring, exposing ~ 0.10 cm² to the H₂SO₄ electrolyte (pH 0.24, 23°C), and cyclic voltammograms are recorded. This procedure ensures a one-to-one correlation between the imaged MoS₂ nanoparticles and the measured activity for hydrogen evolution.
- 22. S. Trasatti, J. Electroanal. Chem. 39, 163 (1972).
- 23. J. K. Nørskov et al., J. Electrochem. Soc. 152, J23 (2005).
- 24. We note that Au atoms along the particle edge also scale with the edge length; however, previous experimental

- and computational studies have shown negligible interaction between the MoS₂ and the support (14, 15). leading us to conclude that such sites would be as inactive as those of the blank samples, prepared without MoS2 deposition.
- 25. In our comparison with Pt(111), we assumed that the observed HER on this surface is dominated by terrace atoms, not defects. This is the consensus in the literature (7).
- 26. N. M. Markovic, B. N. Grgur, P. N. Ross, J. Phys. Chem. B 101, 5405 (1997).
- 27. E. Skúlason et al., Phys. Chem. Chem. Phys. 9, 3241 (2007).; 10.1039/B700099E
- 28. This project was supported by the Danish Strategic Research Council. T.F.J. acknowledges an H. C. Ørsted Postdoctoral Fellowship from the Technical University of Denmark. The Center for Individual Nanoparticle Functionality is supported by the Danish National Research Foundation The Center for Atomic-scale Materials Design is supported by the Lundbeck

Supporting Online Material

www.sciencemag.org/cgi/content/full/317/5834/100/DC1 Materials and Methods SOM Text Fig. S1

Tables S1 and S2

20 February 2007; accepted 16 May 2007 10.1126/science.1141483

Understanding Reactivity at Very Low Temperatures: The Reactions of Oxygen Atoms with Alkenes

Hassan Sabbah, Ludovic Biennier, Ian R. Sims, *Yuri Georgievskii, 2 Stephen J. Klippenstein, 3* Ian W. M. Smith 4*

A remarkable number of reactions between neutral free radicals and neutral molecules have been shown to remain rapid down to temperatures as low as 20 kelvin. The rate coefficients generally increase as the temperature is lowered. We examined the reasons for this temperature dependence through a combined experimental and theoretical study of the reactions of O(3P) atoms with a range of alkenes. The factors that control the rate coefficients were shown to be rather subtle, but excellent agreement was obtained between the experimental results and microcanonical transition state theory calculations based on ab initio representations of the potential energy surfaces describing the interaction between the reactants.

pplication of the CRESU technique (1) has shown that a surprising number of bimolecular reactions between neutral gas-phase species are rapid at very low temperatures. To date, rate coefficients for some 45 neutralneutral reactions have been measured (2, 3), in

some cases at temperatures as low as 13 K (4). All have rate coefficients at 298 K [k(298 K)] that are equal to or exceed $\sim 10^{-11}$ cm³ molecule $^{-1}$ s⁻¹. Moreover, the general trend with temperature is for the rate coefficients to increase as the temperature is lowered.

These observations have led to a reevaluation of the chemistry that occurs in the cold cores (10 to 20 K) of dense, dark interstellar clouds (ISCs), where the majority of interstellar molecules have been identified. Although sequences of ionmolecule reactions initiated by the cosmic rayinduced ionization of H2 clearly play a central role in this chemistry, neutral-neutral reactions are now expected to be more important than previously thought (5). Unfortunately, the kinetic database required for detailed astrochemical modeling (6) is still far from complete. There are many reactions that may occur in ISCs, such as those between pairs of unstable species, for which low-temperature kinetic data neither exist nor are likely to be obtained in the foreseeable future. Theoretical or semi-empirical methods of estimating these rate coefficients are therefore desirable.

Several complementary theoretical treatments (7-9) have been advanced to explain the observed negative temperature dependences of rate coefficients for radical-radical reactions, principally on the basis of the notion of adiabatic capture of the reactants via long-range attractive forces. Although they differ in their details, these treatments all predict large rate coefficients at very low temperatures for radical-radical reactions, where there is generally no barrier on the minimum energy reaction path. In the case of radical-molecule reactions, a key issue is whether a potential energy barrier exists along the minimum energy path from reactants to products: either a real barrier (i.e., a maximum above the energy of the separated reactants) or a "submerged" barrier corresponding to a maximum along the minimum energy path between the shallow minimum associated with a prereaction complex and the products (see below). Further theoretical work, particularly by Georgievskii and Klippenstein (10, 11), has shown that a submerged barrier can serve as a second inner transition state (or bottleneck), because the internal states at this smaller interreactant separation are more widely spaced than at the outer, capture transition state. In these circumstances, the rate of reaction falls below that predicted by capture theories, and a version of microcanonical transi-

¹Institut de Physique de Rennes, Laboratoire PALMS, UMR 6627 du CNRS-Université de Rennes 1, Equipe Astrochimie Expérimentale, Bat. 11c, Campus de Beaulieu, 35042 Rennes Cedex, France. ²Combustion Research Facility, Sandia National Laboratories, Livermore, CA 94551, USA. 3Chemistry Division, Argonne National Laboratory, Argonne, IL 60439, USA. ⁴University Chemical Laboratory, Lensfield Road, Cambridge CB2 1EW, UK.

^{*}To whom correspondence should be addressed. E-mail: ian.sims@univ-rennes1.fr (I.R.S.); sjk@anl.gov (S.J.K.); i.w.m. smith@bham.ac.uk (I.W.M.S.)



Supporting Online Material for

Identification of Active Edge Sites for Electrochemical H₂ Evolution from MoS₂ Nanocatalysts

Thomas F. Jaramillo, Kristina P. Jørgensen, Jacob Bonde, Jane H. Nielsen, Sebastian Horch, Ib Chorkendorff*

*To whom correspondence should be addressed. E-mail: ibchork@fysik.dtu.dk

Published 6 July 2007, *Science* **317**, 100 (2007) DOI: 10.1126/science.1141483

This PDF file includes:

Materials and Methods SOM Text Fig. S1 Tables S1 and S2 References

Supporting Online Material

(1) Materials and Methods

The MoS_2 is deposited onto Au(111) after the crystal has been cleaned by sputter-annealing cycles. Mo is vapor deposited from a thoroughly degassed resistively heated Mo filament. Cleanliness of Au and the purity of Mo is confirmed by XPS and STM. Mo is deposited and post-annealed in a sulfiding atmosphere achieved by leaking H_2S through a directed doser until a chamber pressure of 10^{-7} Torr is reached.

After deposition the $MoS_2/Au(111)$ sample is transferred in vacuum to a second UHV chamber and STM is performed with an Aarhus-type STM ^[S1]. STM images are scanned in constant current mode, and a number of 470 Å x 470 Å, 512 x 512 pixel images are obtained for analysis. The well-known structure of MoS_2 ^[13] is confirmed by atomically resolved images. MoS_2 edge length is found by measuring the edge state length of all particles in each image, and normalizing the sum of these by the area of the analyzed images, resulting in an "edge length unit" of $nm_{MoS2-edge}/nm_{geometric}^2$.

For HER measurements aqueous H_2SO_4 at pH 0.24 (de-aerated with N_2) was used. A platinum mesh counter electrode and a SCE reference electrode were employed. Cyclic voltammograms were measured at 5 mV/s using a PAR VMP2 potentiostat. All data are corrected for a small ohmic drop using impedance spectroscopy.

For MoS₂ samples, an exchange current per site was determined by the slope of the linear fit of exchange current density (A/cm²_{geometric}) versus edge state length (nm_{MoS2-edge}/nm²_{geometric}), resulting in 1.67 x 10^{-20} A/nm_{MoS2-edge} and an R² value of 0.93. The Mo-Mo and S-S distances in MoS₂ are 3.15 Å ^[13], resulting in (1/0.315) sites/nm_{MoS2-edge}. This yields 5.25 x 10^{-21} A/site. This value was then multiplied by the site density of Pt (1.5 x 10^{15} sites/cm²) for a fair comparison to transition metals, resulting in 7.9 x 10^{-6} A/cm², as seen in Table S1.

Turn-over frequencies are calculated in Table S1 from exchange current densities using the following relation:

TOF (s⁻¹) =
$$(i_0, A/cm^2) / [(1.5 \times 10^{15} \text{ sites/cm}^2) (1.602 \times 10^{-19} \text{ C/e}^-) (2 \text{ e}^-/\text{H}_2)]$$

(2) Supporting Text

In addition to using exchange current density as a measure of HER activity, one can also use the current density at a specific overpotential from the polarization curves. In general, this figure of merit is more pertinent on practical devices, such as fuel cells or electrolyzers, whereas exchange current density is a property of more fundamental interest. Fig. S1 exhibits current densities measured at -150 mV overpotential versus (a) area coverage and (b) edge length, analogous to the exchange current density scatter plots in Fig. 3. Fig. S1 affirms the conclusions drawn from Fig. 3: current density is not determined by the MoS_2 area coverage – it is linearly dependent on the MoS_2 edge length.

(3) Supporting Figure

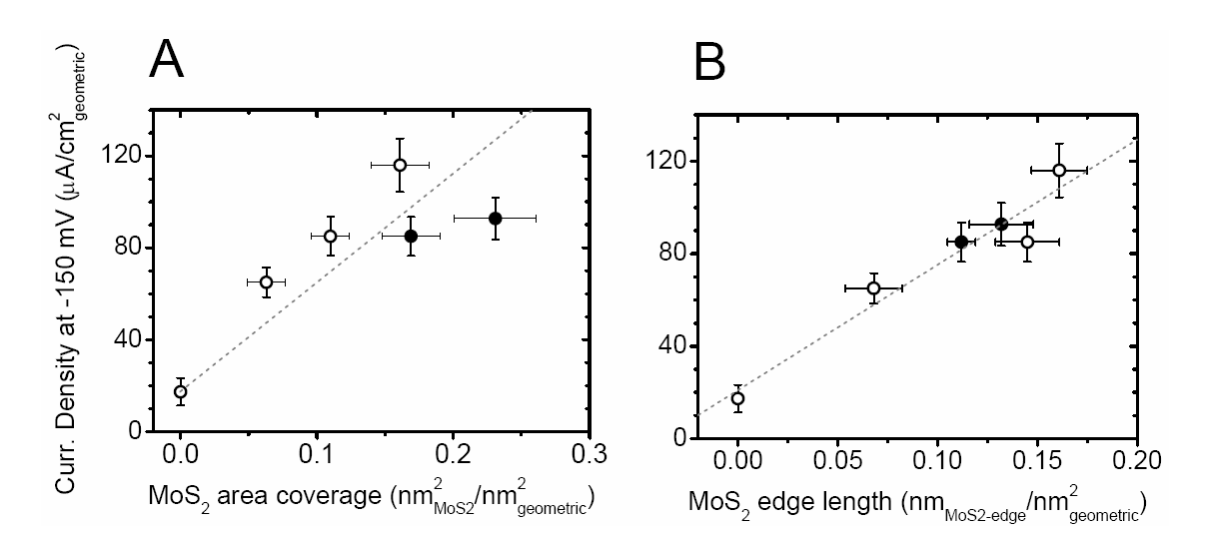


Figure S1. Current density at -150 mV vs. NHE as a function of MoS_2 area coverage (a) and MoS_2 edge length (b). In both figures, open circles are samples annealed to 400 °C, filled circles are samples annealed to 550 °C. The current density does not correlate with the area coverage of MoS_2 , whereas it shows a linear dependence on the MoS_2 edge length. This is further support that the active site for the hydrogen evolution reaction is on the particle edge. The edge length is measured on all imaged particles and normalized by the imaged area, identical to Fig. 3.

(4) Supporting Tables

Material	Exchange current density (A/cm ²), assuming 1.5 x 10 ¹⁵ sites/cm ²	Exchange current pr site (A/site)	TOF (s ⁻¹)
Pt(111)	4.5E-04 ^[25]	3.00E-19	0.94
Hg	5.0E-13 ^[21]	3.34E-28	1.04E-09
MoS ₂ -edge	7.9E-06	5.25E-21	1.64E-02

Table S1. Calculation of TOFs.

Annealing temperature	# islands	tot edge length (nm)	MoS ₂ Area coverage nm ² /nm ²	MoS ₂ Edge length nm/nm ²	Exchange current density A/cm ²	Tafel Slope (mV/decade)	R ² for fitting to Tafel equation
Blank - 400°C	-	-	-	-	9.84E-08	-73.8	> 0.999
400°C	121	845	0.063	0.072	1.26E-07	-55.5	> 0.999
400°C	340	1818	0.110	0.154	2.61E-07	-59.9	> 0.999
400°C	264	1606	0.161	0.171	3.09E-07	-55.2	> 0.999
550°C	181	1648	0.231	0.140	2.18E-07	-56.7	> 0.999
550°C	195	1679	0.169	0.119	1.73E-07	-56.1	> 0.999

Table S2. Analysis of STM images and electrochemical data. Annealing temperature, number of islands imaged, total imaged edge length, MoS_2 area coverage, MoS_2 edge length, exchange current densities and Tafel slopes (and their R^2 values). Total edge length was used rather than the predominant Mo-edge as no significant difference in correlation is observed if the S-edge is excluded.

(5) Supporting References

S1. E. Lægsgaard, F. Besenbacher, K. Mortensen, I. Stensgaard, J. Microsc. 152 663 (1988).